Physical and Gamma Ray Attenuation Properties of Bismuth-Lead-Phosphate Glass

Abo-alqasem S. Mater [1,2,4] * - Rasha A. Mansouri [3,4] - Daefalla M. Tawati [3,4] - Fawzi A. Ikraiam [2,4] - Nagi A. Hussien [3,4]

1 Physics Department , Faculty of Science, Fezzan Univesity , Murzuq, Libya.

2 Physics Department, Faculty of Science, Omar Al–Mukhtar University, El–Beida, Libya.

3 Department of Physics, Faculty of Science, University of Benghazi, Benghazi, Libya.

4 Physics Research Group, Depratment of Physics, Faculty of Science, University of Benghazi, Benghazi, Libya.

ABSTRACT

In this paper, the physical characteristics and radiation attenuation parameters of five ternary (50-x) PbO-xBi$_2$O$_3$-50P$_2$O$_5$ glass samples with different compositions were examined. The physical properties investigated were glass density (ρ), molar volume (V_M), molar volume of oxygen (V_O), and oxygen packing density (OPD). An empirical formula was used to determine the glass density theoretically and compared with the experimental density obtained from the Archimedes method. The comparison yielded reasonable results but did not achieve the desired level of accuracy as expected. The findings revealed that both density and molar volume exhibited an increase with higher Bi$_2$O$_3$ content. However, the molar volume of oxygen (V_O) and oxygen packing density (OPD) show inconsistent behavior, showing a slight increase in V_O and a decrease in OPD. Furthermore, the essential radiation properties, including the coefficient of linear attenuation (LAC), coefficient of mass attenuation (MAC), half-value layer (HVL), and tenth-value layer (TVL), were determined through experimental and theoretical calculations using the NaI (Tl) detection system and the Phy-X/PSD program, respectively. The results indicated reasonable consistency between the two methods, with the Bi16Pb34P50 sample demonstrating superior radiological properties among the samples. Overall, the study illustrated that the addition of bismuth to phosphate and lead glass improved the glass samples' radiation and physical characteristics.

KEYWORDS: density, lead-phosphate glass, oxygen molar volume, oxygen packing density, physical parameters; mass and linear attenuation coefficient.

1. INTRODUCTION

In the past century, glass has drawn a lot of interest for its potential applications in a variety of fields, including research, industry, medicine, and construction. Its many advantages include high transmittance, durability, water resistance, transparency, high homogeneity, and acceptable mechanical and chemical stability [1]. These features exhibited by glass provided it with simple applications and processing. One of the important applications for glass is in the area of shielding and radiation protection. Protection from radiation is needed since radiation is present in many fields like energy generation, medical diagnosis and treatment, and others. These advantages of radiation come with costs and hazards to the environment and health.

To avoid these risks, protection measures are required to lessen the high-energy gamma photons that are radiated from radioactive sources [2]. Traditionally, concrete and lead are primarily used for such protection, shielding, and radiation reduction measures. Concrete was the preferred material due to its high density, easy formability, structural strength and low cost [3]. However, concrete has several disadvantages, namely: cracking, space consumption, opacity to visible light, aggregate expansion, moisture, and a progressive decrease in mechanical strength and density [4]. On the other hand, lead is one of the most commonly used materials for radiation shielding and protection [5]. Nevertheless, the opacity and potential health risks associated with lead toxicity have prompted researchers to seek safer, more environmentally friendly alternatives for radiation shielding. Glass, with its diverse properties, emerges as a promising candidate. By offering superior radiation protection while minimizing environmental concerns, glass could provide a viable solution to the challenges posed by lead-based materials. Borate, silicate, and

*Correspondence: Abo-alqasem S. Mater

Aboalksemmater@gmail.com

phosphate glasses are among the most significant types. Phosphate glass, in particular, exhibits unique properties like high absorption, low glass transition temperature, and minimal optical scattering. While ionizing radiation cannot be completely eliminated, its levels can be reduced [6]. HVL and TVL are commonly measured parameters in shielding calculations where they determine the required material thickness to attenuate gamma radiation intensity to half and tenth of its original amounts, respectively, and are usually stated in mm or cm distance units [7]. The present paper investigates the effect of the addition bismuth oxide on lead phosphate glass with different percentages. The different physical properties, namely: glass density, molar volume (V_M), oxygen molar volume (V_o) and oxygen packing density (OPD), are evaluated. In addition, the radiation shielding specifications for TVL, MAC, HVL, and LAC are also determined. The attenuation coefficient was evaluated in two ways: experimentally using the thallium-activated sodium iodide, NaI (Tl), detection system, and

theoretically using the Phy-X/PSD program, at gamma energies of 0.662, 1.173 and 1.33 MeV.

2. Experiment Methods

2.1. Glass Preparation and Density Determination

Five glass samples with the composition (50-x) PbO-xBi_2O_3-$50P_2O_5$, where x = 0, 4, 8, 12, and 16 mol%, were prepared using the "melt-quenching" technique. Glass sample densities were measured using the Archimedes method with xylene serving as the immersion solvent. The experimental density was calculated using the following relationship [8]:   (1)

Where w_a and w_X represent the sample weight in air and xylene, respectively, and ρ_x denotes the density of xylene (ρ_x = 0.861 g cm^{-3}). The details of the preparation method and the glass density measurement were reported in our previous work [9]. The produced glass samples and their chemical compositions are presented in Table 1 [9].

Table 1: Glass compositions and their photos for prepared samples [9].

Sample code	Chemical composition (mol %)	Prepared glasses
Bi0Pb50P50	$50PbO-0Bi_2O_3-50P_2O_5$	
Bi4Pb46P50	$46PbO-4Bi_2O_3-50P_2O_5$	
Bi8Pb42P50	$42PbO-8Bi_2O_3-50P_2O_5$	
Bi12Pb38P50	$38PbO-12Bi_2O_3-50P_2O_5$	
Bi16Pb34P50	$34PbO-16Bi_2O_3-50P_2O_5$	

2.2. Physical Parameters Related to the Glass Density

The V_M is calculated using the following formula [10]:

$$V_M = \frac{\sum M_i x_i}{\rho_{exp}} \quad (2)$$

Where M_i is the molecular weight of the glass sample and ρ_{exp} is the experimentally evaluated glass sample density.

The oxygen molar volume, V_o (the volume of glass that contains one mole of oxygen) is calculated by the formula [11]:

$$V_o = \frac{V_M}{\sum X_i n_i} \quad (3)$$

Where n_i number of oxygen atoms in each component oxide.

The OPD, which provides information about the tightness of glass network, is determined by [12]:

$$OPD = 1000 \, C \left(\frac{\rho_{exp}}{M}\right) \quad (4)$$

Where C represents the number of oxygen atoms.

2.3. Measurement of Linear Attention Coefficient

In this work, sodium iodide (NaI) detection system was used to determine LAC experimentally. The basic gamma ray detection system, which is shown in Figure 1 and used for spectral measurements, consists of a

"1.5x1.5" crystal of Thallium-activated sodium iodide scintillation detector, NaI (Tl), model no. (PM-9266B) and serial no. (WA00012638), a multichannel analyzer MCA, a high-voltage power supply, and a CASSY sensor. The detector assembly was inserted into a 15-mm-thick cylindrical lead shield to reduce background and unwanted radiation that might come from sources in the lab or from other sources such as natural radionuclides and cosmic rays [13]. Collimated gamma photons from point sources ^{137}Cs (0.662 MeV) and ^{60}Co (1.173, 1.33 MeV) were used in the measurements, and the glass samples were placed between the source and the NaI detector, as shown in Figure 1. Counts of the incident and attenuated intensities of gamma ray energies for each glass sample were recorded for 20 min. The measurements were repeated three times with and without the glass samples for better statistics. The net counts under the photo peaks were obtained after background subtraction and Gaussian fitting of the spectral peaks.

The measured LAC of all glasses was acquired by the Beer-Lambert relation [13]:

$$I = I_0 e^{-(LAC)x} \qquad (5)$$

Where I_0 is the intensity of the incident radiation on the glass sample, I is the intensity of attenuated radiation, and x is the glass sample thickness.

Fig. 1: NaI detection system used in the research.

2.4. Calculation of Mass Attenuation Coefficient (MAC)

MAC values of glass samples were calculated from the determined LAC values in the previous section using the following formula [14]:

$$MAC = \frac{LAC}{\rho_{exp}} \qquad (6)$$

Where ρ_{exp} (g cm^{-3}) is the experimentally measured density of glass samples.

2.5. Determination of Half Value Layer (HVL)

The formula below was utilized to determine HVL values [14]:

$$HVL = \frac{0.693}{LAC} \qquad (7)$$

2.6. Determination of Tenth Value Layer (TVL)

TVL values were calculated using the following formula [14]:

$$TVL = \frac{2.30}{LAC} \qquad (8)$$

3. THEORETICAL STUDY

3.1. Empirical Density

The empirical densities of the glass samples (ρ_{emp}) were found theoretically using the following formula [15]:

$$\rho_{emp} = 0.53 \frac{\sum M_i X_i}{\sum V_i X_i} \qquad (9)$$

Where M_i is the molecular weight of the glass components, X_i is the mole fraction for each component, and V_i is the packing density parameter. For an oxide $M_X O_Y$, the V_i parameter can be determined by:

$$V_i = \frac{4}{3} \pi NA (X.r_M^3 + Y.r_O^3) \qquad (10)$$

Where r_M and r_O are the ionic radii of metal and oxygen, N_A is the Avogadro number, and X and Y are the number of metal and oxygen atoms, respectively.

3.2. Theoretical Calculations of Radiation Parameters

The radiation parameters LAC, MAC, HVL, and TVL were established theoretically by Phy-X/PSD software [16]. ^{137}Cs, and ^{60}Co gamma radioactive sources were selected for this program.

4. Results and discussion

4.1. Outcomes of Physical Characteristics

Glass density (ρ), V_M, V_O, and OPD, are the most important physical properties that were studied in this current work. Density measurement is a convenient way to sense any structural difference in the glassy system, since density is affected by changes in atomic coordination numbers and the size of the ionic radius in the glass lattice. When experimental density (ρ_{exp}) and theoretical density (ρ_{emp}) were determined, it was observed that they increase linearly with increasing Bi$_2$O$_3$ concentration, as shown in Table 2 and Figures 2 and 3 with a deviation (RD%) ranging from 9.02 to 13.72%. This deviation is not closely agreed upon but is reasonable compared to previous published results for different glass compositions calculated by several methods [17][18] [19].This may be due to the effect of bismuth and lead on the structural composition of the glass samples compared to other oxide. This may also be attributed to Inaba and Fujino who has neglected to include lead and bismuth data with the phosphate glass when calculating the theoretical density. As for the increase in density with increasing Bi$_2$O$_3$, Bi$_2$O$_3$ (M =

465.959 g mol⁻¹) was replaced by PbO (M = 223.199 g mol⁻¹) in the composition, which resulted in obtaining denser glass samples. Values of molar volume have increased from 37.48 cm³ mol⁻¹ to 43.68 cm³ mol⁻¹ as the Bi_2O_3 content of the glass matrix increased, as shown in Figure 4. This suggests a potential expansion of the vitreous network and a more open vitreous structure in the glassy matrix. In general, molar volume of any glassy matrix increases with increasing number of oxygen atoms and the size of ionic radii [17].

Table 2: Physical Parameters of the glass system xBi₂O₃–(50 – x)PbO–50P₂O₅

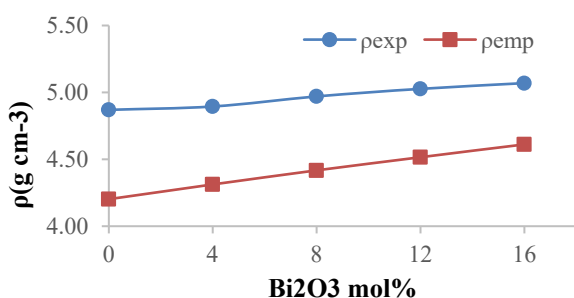| Sample code	ρ$_{exp}$[9] (g/cm³)	ρ$_{emp}$ (g/cm³)	RD%	M (mol/g)	V$_M$[9] (cm³/mol)	V$_O$ (cm³/mol)	OPD (mol/L)
S1	4.87	4.20	13.72	182.57	37.48	12.49	80.02
S2	4.89	4.31	11.90	192.28	39.28	12.75	78.40
S3	4.97	4.42	11.13	201.99	40.64	12.86	77.75
S4	5.03	4.52	10.15	211.70	42.11	12.99	76.93
S5	5.07	4.61	9.02	221.41	43.68	13.16	76.00

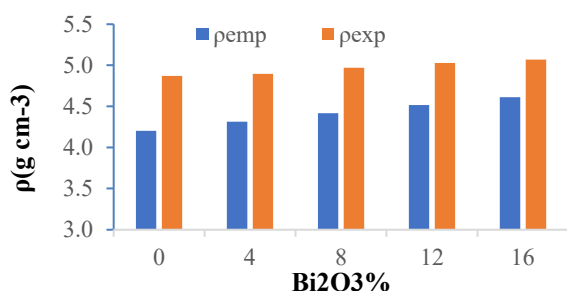**Fig 2: The experimental and empirical densities as a function of Bi₂O₃ mol% content.**

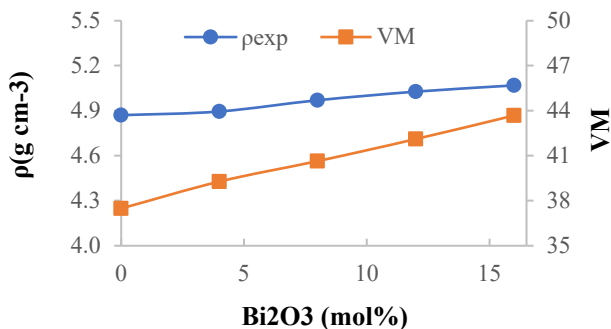**Fig 3: A histogram of the experimental and the empirical densities.**

Fig 4: Variation of ρ$_{exp}$ and V$_M$ with Bi₂O₃ mol% content.

The relationship between the OPD and the V_o greatly affects the physical properties of the glass; through the oxygen packing density, the rigidity of OPD in the glass network is known. There is an inverse relationship between OPD and V_o and this inverse general behavior is experimentally confirmed by the results shown in Table 2 and Figure 5. This behavior indicates a bond decrease in the glass matrix as the glass structure becomes tighter and more rigid [20].
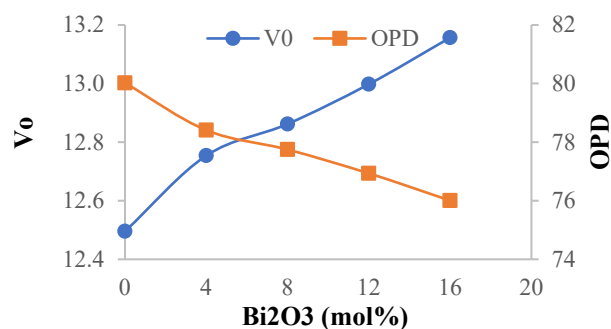

Figure 5: Variation of V$_O$ and OPD with Bi₂O₃ mol% content.

4.2 Radiation Properties

LAC and MAC are critical factors in evaluating a material's ability to attenuate gamma radiation. LAC determines how well a material reduces radiation intensity per unit thickness, while MAC measures the reduction in intensity per unit mass [21]. The LAC and MAC for the glass samples were determined experimentally and theoretically, experimentally using a sodium iodine detection system and theoretically using Phy-X/PSD program at the specified energies of 0.662, 1.17, and 1.33 MeV. The results are shown in Tables 3 and 4. Ahigh degree of concordance was observed

between the two methods, indicating that tabulation-based electronic programs are reliable tools for determining attenuation coefficients. For the gamma energies 0.662 MeV, 1.17 MeV and 1.33 MeV used, the highest LAC and MAC values of to 0.478 cm^{-1} and 0.0944 cm^2/g respectively, were found at the 0.662 MeV energy, and in the sample, Bi16Pb34P50, containing 16 mol% of Bi_2O_3. Moreover, the lowest LAC and MAC

values of 0.436 cm^{-1} and 0.0896 cm^2/g, respectively, were found at value at 1.33 MeV energy, and in the sample, Bi0Pb50P50, containing 0 mol% of Bi_2O_3 as shown in Figures 6, 7, 9, and 10. The LAC and MAC values increased with increasing Bi_2O_3 concentration at each of the gamma energies 0.662, 1.17 and 1.33 MeV, as shown in Figures 8 and 11.

Table 3: Comparison of MAC values calculated experimentally and values by the Phy-X code of the glass system xBi₂O₃– (50 – x) PbO–50P₂O₅

MAC (cm²/g)								
0.662 MeV			1.173 MeV			1.33 MeV		
EXP	Phy-x	RD%	EXP	Phy-x	RD%	EXP	Phy-x	RD%
0.0896	0.0956	6.26	0.0541	0.0602	10.18	0.0528	0.0554	4.64
0.0910	0.0963	5.57	0.0549	0.0603	8.98	0.0530	0.0555	4.56
0.0907	0.0970	6.46	0.0589	0.0604	2.60	0.0535	0.0556	3.82
0.0928	0.0976	4.85	0.0638	0.0606	-5.29	0.0574	0.0557	-3.18
0.0944	0.0981	3.83	0.0638	0.0607	-5.25	0.0594	0.0557	-6.61

Table 4: Comparison between the LAC values calculated experimentally and values obtained by the Phy-X code of the glass system xBi₂O₃– (50 – x) PbO–50P₂O₅

MAC (cm2/g)								
0.662 MeV			1.173 MeV			1.33 MeV		
EXP	Phy-x	RD%	EXP	Phy-x	RD%	EXP	Phy-x	RD%
0.436	0.466	6.26	0.263	0.293	10.18	0.257	0.270	4.64
0.445	0.471	5.57	0.269	0.295	8.98	0.259	0.272	4.56
0.451	0.482	6.46	0.293	0.300	2.60	0.266	0.276	3.82
0.467	0.490	4.85	0.321	0.304	-5.29	0.289	0.280	-3.18
0.478	0.497	3.83	0.324	0.307	-5.25	0.301	0.283	-6.61
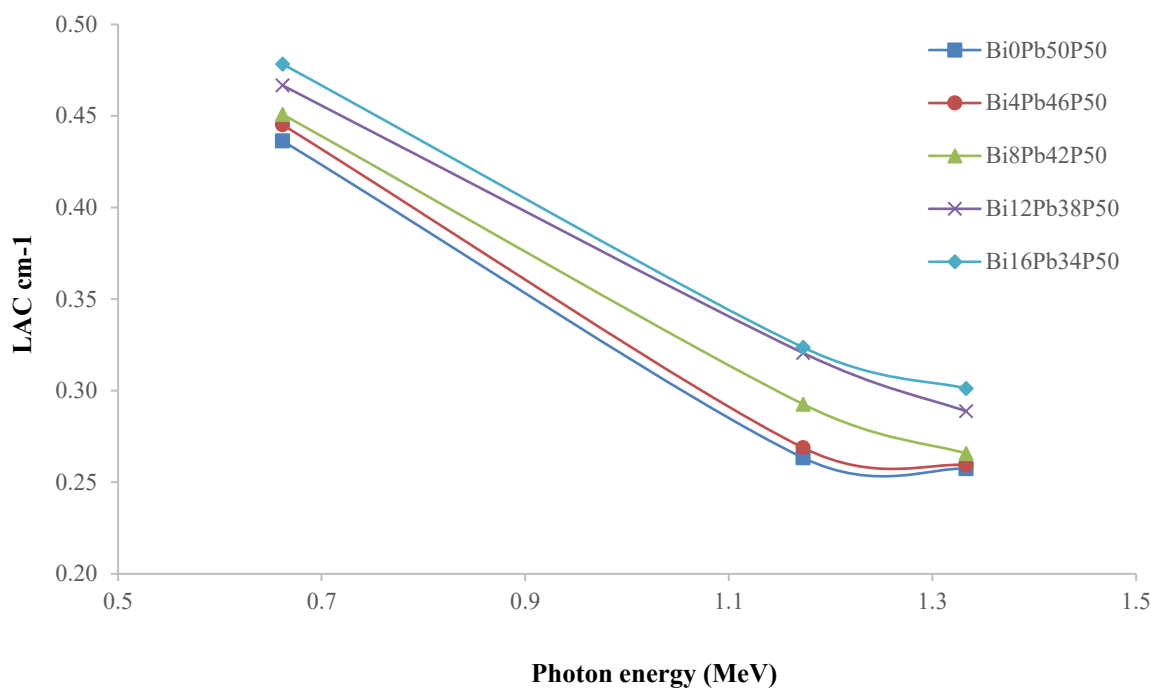
Fig 6: The relationship between linear attenuation coefficient (cm^{-1}) and photon energy for Bi$_2$O$_3$-PbO-P$_2$O$_5$ glasses (experimentally).
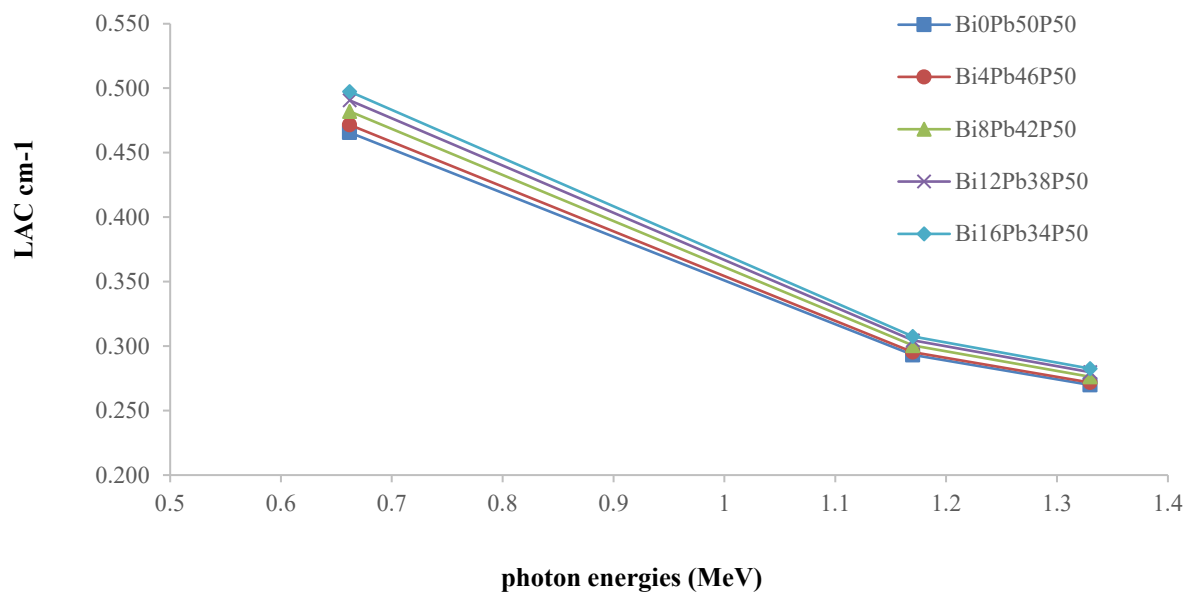
Fig 7: The relationship between linear attenuation coefficient (cm^{-1}) and photon energy for Bi$_2$O$_3$-PbO-P$_2$O$_5$ glasses (theoretically).
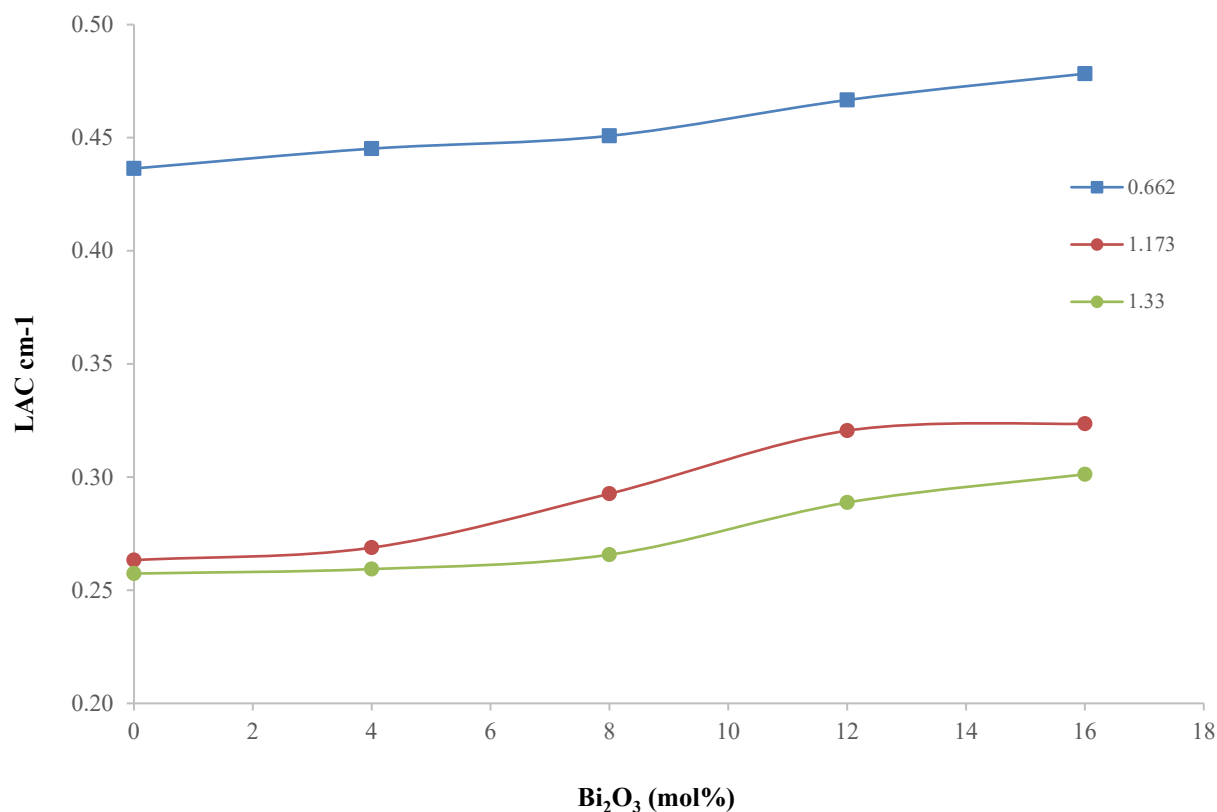
Fig 8: The relationship between linear attenuation coefficient (cm^{-1}) and Bi$_2$O$_3$ (mol%) content for Bi$_2$O$_3$-PbO-P$_2$O$_5$ glasses at different photon energies (experimentally).
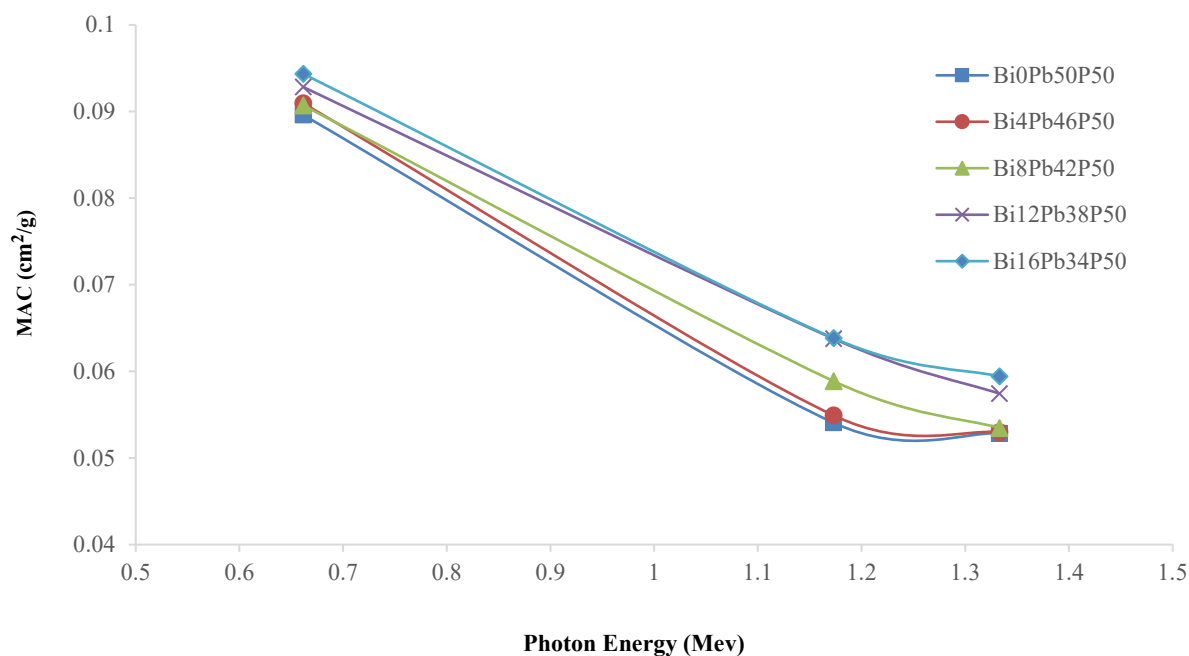
Fig 9: The relationship between mass attenuation coefficient (cm^2/g) and photon energy for Bi$_2$O$_3$-PbO-P$_2$O$_5$ glasses (experimentally).
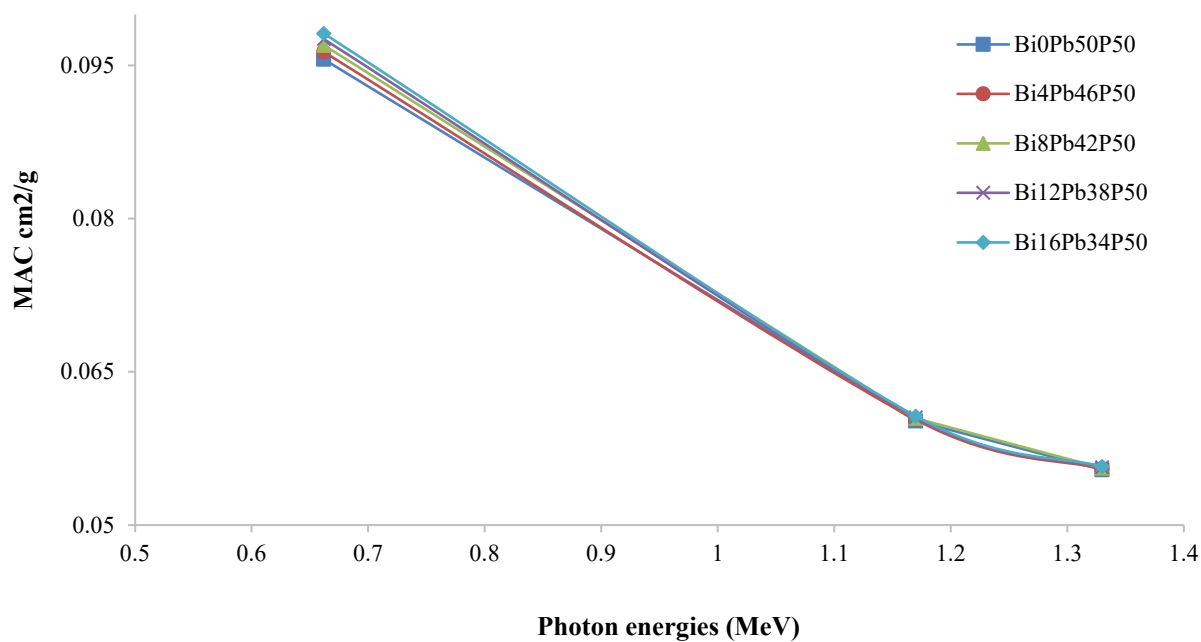
Fig 10: The relationship between mass attenuation coefficient (cm²/g) and photon energy for Bi₂O₃-PbO-P₂O₅ glasses (theoretically).
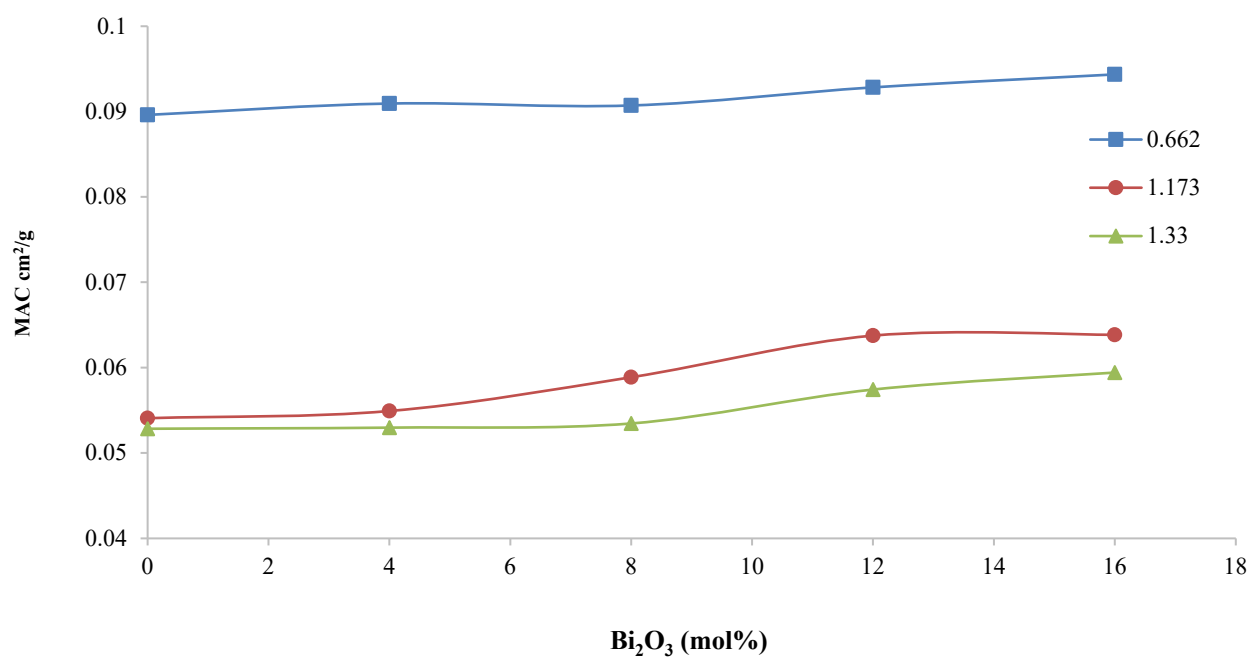
Fig 11: The relationship between mass attenuation coefficient (cm²/g) and Bi₂O₃ (mol%) content for Bi₂O₃-PbO-P₂O₅ glasses at different photon energies (experimentally).

Half-Value Layer (HVL) and Tenth-Value Layer (TVL) are crucial metrics for understanding the radiation shielding capabilities of glass. HVL indicates the thickness of material required to reduce radiation intensity by half, while TVL represents the thickness needed to reduce it by a factor of ten [19]. In the context of the prepared glass samples, the decrease in the HVL percentage indicates a decrease in the thickness required to reduce the radiation capacity by half, and this decrease appeared in the results shown in Table 5 and Figures 12 and 14, which represented HVL against energy and Figure 16, which represented HVL against concentration,

and the best and the lowest thickness of the prepared glass samples was Bi16Pb34P50 sample. The highest HVL thickness was for the sample Bi0Pb50P50. At all specified energies, TVL values were in complete agreement with the maximum and the minimum HVL thickness of the samples, as shown in Table and Figures 13 and 15. In other words, the addition of Bi_2O_3 and the reduction of PbO greatly enhance the shielding ability of the glasses and significantly reduce the necessary sample thickness, which is both practical and economical, as shown in Figure 17

Table 5: Comparison between the HVL values calculated experimentally and values obtained by the Phy-X code of the glass system xBi_2O_3– (50 – x) PbO–50P_2O_5

HVL (cm)								
0.662 MeV				1.173 MeV			1.33 MeV	
EXP	Phy-x	RD%	EXP	Phy-x	RD%	EXP	Phy-x	RD%
1.588	1.489	6.26	2.632	2.364	10.18	2.693	2.568	4.64
1.557	1.470	5.57	2.579	2.347	8.98	2.673	2.551	4.56
1.537	1.438	6.46	2.369	2.307	2.60	2.608	2.509	3.82
1.485	1.413	4.85	2.162	2.277	-5.29	2.401	2.477	-3.18
1.449	1.394	3.83	2.142	2.254	-5.25	2.301	2.453	-6.61

Table 6: Comparison between the TVL values calculated experimentally and values obtained by the Phy-X code of the glass system xBi_2O_3– (50 – x) PbO–50P_2O_5

TVL (cm)								
0.662 MeV				1.173 MeV			1.33 MeV	
EXP	Phy-x	RD%	EXP	Phy-x	RD%	EXP	Phy-x	RD%
5.277	4.946	6.26	8.744	7.854	10.18	8.947	8.532	4.64
5.172	4.884	5.57	8.566	7.797	8.98	8.880	8.474	4.56
5.107	4.777	6.46	7.868	7.664	2.60	8.665	8.334	3.82
4.934	4.694	4.85	7.184	7.564	-5.29	7.974	8.228	-3.18
4.814	4.630	3.83	7.116	7.489	-5.25	7.645	8.150	-6.61
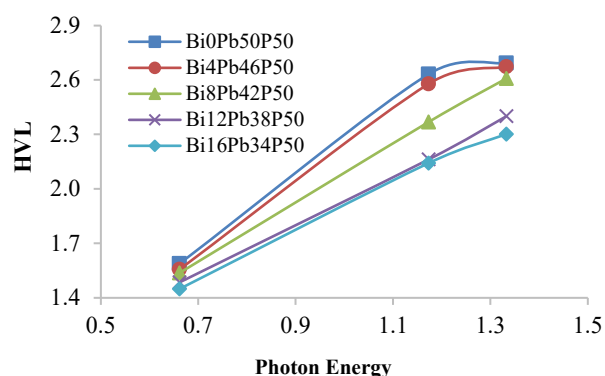
Fig 12: The relationship between half-value layer (cm) and photon energy for Bi$_2$O$_3$-PbO-P$_2$O$_5$ glasses at different photon energies (experimentally).
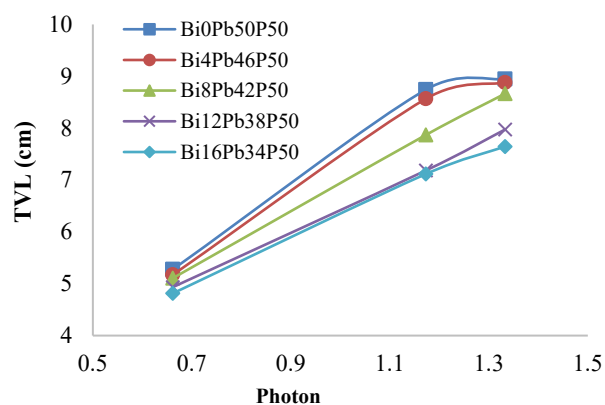
Fig 13: The relationship between tenth value layer (cm) and photon energy for Bi$_2$O$_3$-PbO-P$_2$O$_5$ glasses at different photon energies (experimentally).
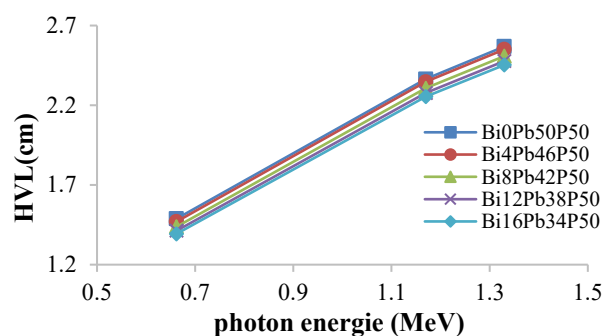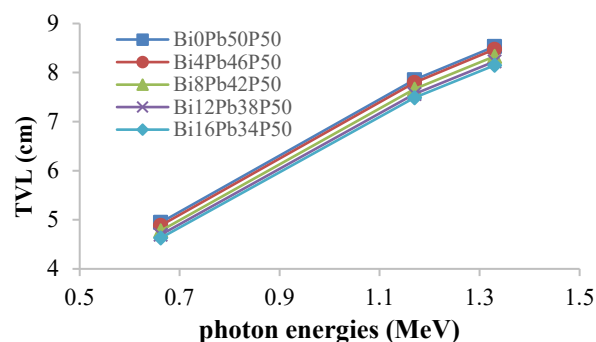

Fig 14: The relationship between half-value layer (cm) and photon energy for Bi$_2$O$_3$-PbO-P$_2$O$_5$ glasses at different photon energies (theoretically).
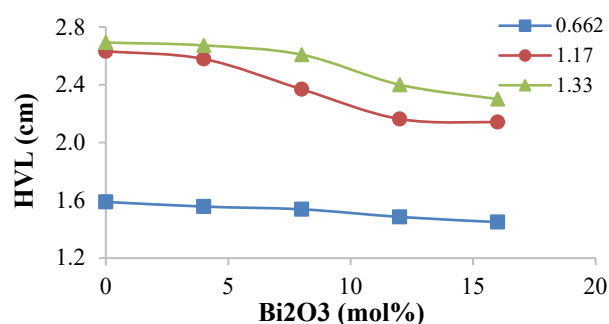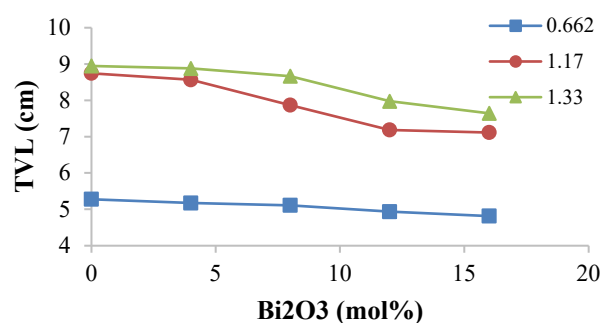

Fig 15: The relationship between tenth value layer (cm) and photon energy for Bi$_2$O$_3$-PbO-P$_2$O$_5$ glasses at different photon energies (theoretically).

Fig 16: The relationship between half-value layer (cm) and Bi$_2$O$_3$ (mol%) content for Bi$_2$O$_3$-PbO-P$_2$O$_5$ glasses (experimentally).

Fig 17: The relationship between tenth value layer (cm) and Bi$_2$O$_3$ (mol%) content for Bi$_2$O$_3$-PbO-P$_2$O$_5$ glasses (experimentally).

5. CONCLUSION

The goal of this research was to investigate the physical characteristics of phosphate, lead, and bismuth glasses, focusing on how these properties vary with changes in concentration. The comparison of theoretical and experimental methods for estimating the density of glass samples produced a satisfactory result. The results showed that as Bi_2O_3 levels increased, so did density and molar volume, indicating that the glassy networks expanded and the glassy structure became more open within the glassy matrix. The response of oxygen molar volume (V_O) and OPD was contradictory; there was a slight increase in V_O, but this was offset by a decrease in OPD. This means that as the matrix's connections decrease, the glass structure becomes more compact. The LAC was also measured experimentally with three gamma energies: 0.662, 1.117, and 1.33 MeV from radioactive point sources ^{137}Cs and ^{60}Co and a NaI(Tl) scintillation detection system. LAC and MAC then calculated theoretically, along with HVL and TVL by the Phy-X/PSD program at the same energies, and the experimental and theoretical findings were contrasted, and there was good agreement between the two results. LAC and MAC results indicated that the inclusion of Bi_2O_3 increased glass sample radiation attenuation capacity. Similarly, the best results in HVL and TVL were obtained in the sample Bi16Pb34P50, which contained the highest concentration of Bi_2O_3.

REFERENCES

1. Algradee MA, Saleh EE, Sherbini TM, El Mallawany R. Optical and gamma-ray shielding features of Nd3+ doped lithium-zinc-borophosphate glasses. Optik, (2021), 242:167059.

   https://doi.org/10.1016/j.ijleo.2021.167059

2. Singh S, Kaur R, Rani S, Sidhu BS. Investigations on physical, structural and nuclear radiation shielding behaviour of niobium–bismuth–cadmium–zinc borate glass system. Progress in Nuclear Energy. 2021 Dec 1;142:104038.

   https://doi.org/10.1016/j.pnucene.2021.104038

3. Nabil IM, El-Samrah MG, Omar A, Tawfic AF, El Sayed AF. Experimental, analytical, and simulation studies of modified concrete mix for radiation shielding in a mixed radiation field. Scientific Reports. 2023 Oct 17;13(1):17637.

   https://doi.org/10.1038/s41598-023-44978-8

4. Bagheri R, Adeli R. Gamma-ray shielding properties of phosphate glasses containing Bi2O3, PbO, and BaO in different rates. Radiation Physics and Chemistry. 2020 Sep 1;174:108918.

   https://doi.org/10.1016/j.radphyschem.2020.108918

5. Tamam N, Alrowaili ZA, Hammoud A, Lebedev AV, Boukhris I, Olarinoye IO, Al-Buriahi MS. Mechanical, optical, and gamma-attenuation properties of a newly developed tellurite glass system. Optik. 2022 Sep 1;266:169355.

   https://doi.org/10.1016/j.ijleo.2022.169355

6. Kumar A, Sayyed MI, Dong M, Xue X. Effect of PbO on the shielding behavior of ZnO–P2O5 glass system using Monte Carlo simulation. Journal of Non-crystalline Solids. 2018 Feb 1;481:604-7.

   https://doi.org/10.1016/j.jnoncrysol.2017.12.001

7. Akkaş A. Determination of the tenth and half value layer thickness of concretes with different densities. Acta Physica Polonica A. 2016 Apr;129(4):770-2.

   https://doi.org/10.12693/APhysPolA.129.770

8. Azianty S, Yahya AK. Enhancement of elastic properties by WO3 partial replacement of TeO2 in ternary (80− x) TeO2‑20PbO‑xWO3 glass system. Journal of non-crystalline solids. 2013 Oct 15;378:234-40.

   https://doi.org/10.1016/j.jnoncrysol.2013.07.016

9. Seham Y. M. Dogharsham, Ollaa M. Mailoud, Abo-alqasem S. Mater, Daefalla M. Tawati, Fawzi A. Ikraiam. Mechanical Properties of Ternary Bi2O3–PbO–P2O5 Glasses. Accepted in the 1st international Conference on Mechanical Engineering, Material and Renewable Energy. Faculty of Engineering, University of Benghazi, Benghazi –Libya.

10. Abd-Allah WM, Saudi HA, Shaaban KS, Farroh HA. Investigation of structural and radiation shielding properties of 40B 2 O 3–30PbO–(30-x) BaO-x ZnO glass system. Applied Physics A. 2019 Apr;125:1-0.

    https://doi.org/10.1007/s00339-019-2574-0

11. Ersundu MÇ, Ersundu AE, Gedikoğlu N, Şakar E, Büyükyıldız M, Kurudirek M. Physical, mechanical and gamma-ray shielding properties of highly transparent ZnO-MoO3-TeO2 glasses. Journal of Non-Crystalline Solids. 2019 Nov 15;524:119648.

    https://doi.org/10.1016/j.jnoncrysol.2019.119648

12. Kaur P, Singh KJ, Thakur S, Singh P, Bajwa BS. Investigation of bismuth borate glass system modified with barium for structural and gamma-ray shielding properties. Spectrochimica Acta Part A: Molecular and Biomolecular Spectroscopy. 2019 Jan 5;206:367-77.

    https://doi.org/10.1016/j.saa.2018.08.038

13. Knoll G. F., "Radiation Detection and Measurement," 4th Edition, John Wiley & Sons, New York, 2010.

14. Coşkun A, Çetin B. The Effect of Lead Oxide on the Change in Gamma Ray Protection Parameters of Bismuth Oxide. Avrupa Bilim ve Teknoloji Dergisi. 2023(47):18-21.

    https://doi.org/10.31590/ejosat.1234613

15. Inaba S., Fujino S. Empirical equation for calculating the density of oxide glasses. Journal of the American Ceramic Society. 2010 Jan;93(1):217-20.

   https://doi.org/10.1111/j.1551-2916.2009.03363.x

16. Şakar E, Özpolat ÖF, Alım B, Sayyed MI, Kurudirek M. Phy-X/PSD: development of a user-friendly online software for calculation of parameters relevant to radiation shielding and dosimetry. Radiation Physics and Chemistry. 2020 Jan 1;166:108496.

   https://doi.org/10.1016/j.radphyschem.2019.108496

17. Abo-alqasem S, Abdelrahman SA, Tawati DM, Ikraiam FA, Hussein NA, Basil SS. Physical Properties of Bi2O3–PbO–P2O5 Glasses. Alq. J. Med. App. Sci., Special Issue for 6th International Conference in Basic Science and Their Applications (6th ICBSTA, 2023), P: 303 – 313, 2/12/2023

18. Mostafa AG, Saudi HA, Hassaan MY, Salem SM, Mohammad SS. Studies on the shielding properties of transparent glasses prepared from rice husk silica. American Journal of Modern Physics. 2015;4(4):149-57.

   https://doi.org/10.11648/j.ajmp.20150404.11

19. Singh S, Kaur R, Rani S, Sidhu BS. Investigations on physical, structural and nuclear radiation shielding behaviour of the niobium-bismuth-cadmium–zinc borate glass system. Progress in Nuclear Energy. 2021 Dec 1;142:104038.

   https://doi.org/10.1016/j.pnucene.2021.104038

20. Sayyed MI, Kaky KM, Gaikwad DK, Agar O, Gawai UP, Baki SO. Physical, structural, optical and gamma radiation shielding properties of borate glasses containing heavy metals (Bi2O3/MoO3). Journal of Non-Crystalline Solids. 2019 Mar 1;507:30-7.

   https://doi.org/10.1016/j.jnoncrysol.2018.12.010

21. Dahinde PS, Dapke GP, Raut SD, Bhosale RR, Pawar PP. Analysis of half value layer (HVL), tenth value layer (TVL) and mean free path (MFP) of some oxides in the energy range of 122KeV to 1330KeV. Indian Journal of Scientific Research. 2019;9(2):79-84.

   https://doi.org/10.32606/IJSR.V9.I2.00014